Chapter 6

Nonlinear control technique for dual combination synchronization of complex chaotic systems

6.1 Introduction

Dynamical systems play a key role in studying different phenomena that undergo spatial and temporal evolutions. The area of studying dynamical systems has attracted much attention and lot of research activities are going in recent years (Liu et al. (2016)). System parameters' changes, broad Fourier transform spectra, fractal properties of the motion in phase plane, and strange attractors are all special characteristics for the chaotic system.

Synchronization of complex chaotic systems is achieving by many techniques have been proposed to design proper controllers, including active control technique (Yassen (2005)), backstepping design (Zhang et al. (2000),), nonlinear control method (Chen and Han (2003)), etc. In this article, a simple but an efficient method viz., nonlinear control method is applied to achieve synchronization of complex chaotic systems using the Lyapunov stability theory. An illustrative example is given to design the procedure and advantage of the result derived.

Most of the previous studies were based on synchronization between one drive and one response systems. After proposing the dual synchronization scheme for one-dimensional

The contents of this chapter have been communicated in ***Nonlinear Dynamics****.*

discrete chaotic systems by Liu and Davis (2000), many researchers found interest and extend their works, and also applied for continuous chaotic systems of higher dimensions (Shahverdiev et al. (2003), Ning et al. (2007), Ghosh and Chowdhury (2010),). In dual synchronization, a pair of drive systems is synchronized with another pair of response systems by using a signal generated through a linear combination of the systems state. Rungi et al. (2011) proposed the combination synchronization scheme, in which two drive systems synchronized with one response system. Zhou et al. (2013) investigated combination synchronization among three nonlinear complex hyper-chaotic systems. The Chinese scientist J. Sun and his co-workers extended the combination synchronization scheme (2013) and the compound synchronization (2014) to achieve synchronization between four chaotic systems. Recently, Sun et al. (2016c) proposed compound-combination synchronization scheme for five chaotic systems, while compound-combination anti-synchronization scheme for five simplest memristor chaotic systems was studied by Sun and Shen (2016). The dual combination synchronization between identical systems was reported in Sun et al. (2016a) to illustrate the effectiveness of the proposed scheme. Therefore, there is enough scope to improve and extend their idea for more security in communication theory, stability analysis, better understanding of the scheme and also other reasons. Therefore till date, there is enough scope to address these types of challenging issues due to consisting of different structures and parameter mismatch of the six different chaotic systems. To apply this method in synchronization of a number of chaotic systems it needs more meaningful improvement during demonstration of the scheme. This has motivated the author to investigate the dual combination synchronization for the six different complex chaotic systems which has not yet been explored much.

6.2 The scheme for dual combination synchronization

A systematic scheme for dual combination synchronization among four drive and two response complex chaotic systems is designed in this section. Let the first two drive systems are

$$\dot{X}_1 = F_1(X_1), \tag{6.1}$$

$$\dot{X}_2 = F_2(X_2), \tag{6.2}$$

where $X_1 = [x_{11}, x_{12}, \cdots, x_{1n}]^T$ and $X_2 = [x_{21}, x_{22}, \cdots, x_{2m}]^T$ are the two state complex vectors of uncoupled drive systems (6.1) and (6.2) ; $F_1 : C^n \to C^n$ and $F_2 : C^m \to C^m$ are the two known complex vector valued functions. The coupled drive system M_1 generates a complex vector signal in the form

$$M_1 = [a_{11}x_{11},\ a_{12}x_{12},\ ...,\ a_{1n}x_{1n},\ a_{21}x_{21},\ a_{22}x_{22},\ ...,\ a_{2m}x_{2m}]^T$$

$$= \begin{bmatrix} A_1 & 0 \\ 0 & A_2 \end{bmatrix} \begin{bmatrix} X_1 \\ X_2 \end{bmatrix} = AX\ , \tag{6.3}$$

where $A_1 = diag[a_{11}, a_{12}, \cdots, a_{1n}]$ and $A_2 = diag[a_{21}, a_{22}, \cdots, a_{2m}]$ are the two known matrices; a_{1i} and a_{2j} cannot be zero simultaneously $(i = 1, 2, \cdots, n,\ \ j = 1, 2, \cdots, m)$; $A = diag[A_1\ ,\ A_2]$; and $X = [X_1^T\ ,\ X_2^T]^T$.

The two drive systems are taken as

$$\dot{Y}_1 = G_1(Y_1), \tag{6.4}$$

$$\dot{Y}_2 = G_2(Y_2), \tag{6.5}$$

where $Y_1 = [y_{11}, y_{12}, \cdots, y_{1n}]^T$ and $Y_2 = [y_{21}, y_{22}, \cdots, y_{2m}]^T$ are the two state complex vectors of the uncoupled drive systems (6.4) and (6.5); $G_1 : C^n \to C^n$ and $G_2 : C^m \to C^m$

are the two known complex vector valued functions. Hence the coupled drive system M_2 generates a complex vector signal in the form

$$M_2 = [b_{11}y_{11},\ b_{12}y_{12},\ \cdots, b_{1n}y_{1n},\ b_{21}y_{21},\ b_{22}y_{22},\cdots,\ b_{2m}y_{2m}]^T$$

$$= \begin{bmatrix} B_1 & 0 \\ 0 & B_2 \end{bmatrix} \begin{bmatrix} Y_1 \\ Y_2 \end{bmatrix} = BY\ , \tag{6.6}$$

where $B_1 = diag\left[b_{11}, b_{12}, \cdots, b_{1n}\right]$ and $B_2 = diag\left[b_{21}, b_{22}, \cdots, b_{2m}\right]$ are the two known matrices; b_{1i} and b_{2j} cannot be zero at the same time $\left(i = 1,2,\cdots,n,\ \ j = 1,2,\cdots,m\right)$; $B = diag[B_1\ ,\ B_2]$; and $Y = [Y_1^T\ ,\ Y_2^T]^T$.

Next let us consider two response systems as

$$\dot{Z}_1 = H_1(Z_1) + U_1\ , \tag{6.7}$$

$$\dot{Z}_2 = H_2(Z_2) + U_2\ , \tag{6.8}$$

where $Z_1 = [z_{11}, z_{12}, \cdots, z_{1n}]^T$ and $Z_2 = [z_{21}, z_{22}, \cdots, z_{2m}]^T$ are the complex state vectors of two uncoupled response systems (6.7) and (6.8); $H_1 : C^n \to C^n$ and $H_2 : C^m \to C^m$ are the two known complex vector valued functions; $U_1 : C^n \times C^n \times C^n \to C^n$ and $U_2 : C^m \times C^m \times C^m \to C^m$ are controller vector valued functions to be designed later. The coupled response system S_1 generates a complex vector signal in the form

$$S_1 = [c_{11}z_{11},\ c_{12}x_{12},\ \cdots,\ c_{1n}z_{1n},\ c_{21}z_{21},\ c_{22}z_{22},\cdots,\ c_{2m}z_{2m}]^T$$

$$= \begin{bmatrix} C_1 & 0 \\ 0 & C_2 \end{bmatrix} \begin{bmatrix} Z_1 \\ Z_2 \end{bmatrix} = CZ\ , \tag{6.9}$$

where $C_1 = diag\left[c_{11}, c_{12}, \cdots, c_{1n}\right]$ and $C_2 = diag\left[c_{21}, c_{22}, \cdots, c_{2m}\right]$ are the two known matrices; c_{1i} and c_{2j} cannot be zero at the same time $\left(i = 1, 2, \cdots, n, \quad j = 1, 2, \cdots, m\right)$; $C = diag[C_1 \ , \ C_2]$; and $Z = [Z_1^T \ , \ Z_2^T]^T$.

The error vector signal for dual combination synchronization is defined as

$$e = P M_1 + Q M_2 - R S_1 \ ,$$

where P, Q and R are three scaling matrices.

For convenience, let us assume P, Q and R are diagonal matrices. Then $e(t)$ is reduced to

$$e = \begin{bmatrix} P_1 A_1 X_1 + Q_1 B_1 Y_1 - R_1 C_1 Z_1 \\ P_2 A_2 X_2 + Q_2 B_2 Y_2 - R_2 C_2 Z_2 \end{bmatrix}, \tag{6.10}$$

where $P = diag\,[P_1 \ , \ P_2]$, $Q = diag\,[Q_1 \ , \ Q_2]$, and $R = diag\,[R_1 \ , \ R_2]$.

Definition 6.1 Dual combination synchronization of the drive systems (6.1), (6.2), (6.4) and (6.5), and the response systems (6.7) and (6.8) are achieved if $\lim_{t \to \infty} \left\| e(t) \right\| = 0$, where $\left\| \cdot \right\|$ denotes matrix norm.

6.3 Stability analysis

In this section, the stability of the scheme for dual combination synchronization is studied. In order to complete our aim, let us design the controller function $U = [U_1^T \ , \ U_2^T]^T$ as

$$U_1 = -H_1(Z_1) + C_1^{-1} R_1^{-1} P_1 A_1 F_1(X_1) + C_1^{-1} R_1^{-1} Q_1 B_1 G_1(Y_1) + k_1 C_1^{-1} R_1^{-1} e_1 \ ,$$

$$U_2 = -H_2(Z_2) + C_2^{-1} R_2^{-1} P_2 A_2 F_2(X_2) + C_2^{-1} R_2^{-1} Q_2 B_2 G_2(Y_2) + k_2 C_2^{-1} R_2^{-1} e_2 \ , \quad (6.11)$$

where $e = [e_1^T \ , \ e_2^T]^T$, k_1 and k_2 are two constants.

Theorem 6.2 Dual combination synchronization of the considered systems is achieved if $k_1 > 0$ and $k_2 > 0$.

Proof: The time derivative of the Equation (6.10) is given by

$$\dot{e} = \begin{bmatrix} P_1 A_1 \dot{X}_1 + Q_1 B_1 \dot{Y}_1 - R_1 C_1 \dot{Z}_1 \\ P_2 A_2 \dot{X}_2 + Q_2 B_2 \dot{Y}_2 - R_2 C_2 \dot{Z}_2 \end{bmatrix},$$

therefore, the error system is obtained as

$$\dot{e} = \begin{bmatrix} P_1 A_1 [F_1(X_1)] + Q_1 B_1 [G_1(Y_1)] - R_1 C_1 [H_1(Z_1) + U_1] \\ P_2 A_2 [F_2(X_2)] + Q_2 B_2 [G_2(Y_2)] - R_2 C_2 [H_2(Z_2) + U_2] \end{bmatrix}. \quad (6.12)$$

Lyapunov candidate function is designed as

$$V = \frac{1}{2} e^T e \ ,$$

whose time derivative can be written as

$$\dot{V} = \frac{1}{2} \dot{e}^T e + \frac{1}{2} e^T \dot{e} \ . \quad (6.13)$$

Equation (6.13) with the aid of Equations (6.11) and (6.12) reduce to

$$\dot{V} = \frac{1}{2} \begin{bmatrix} -k_1 e_1^T, & -k_2 e_2^T \end{bmatrix} \begin{bmatrix} e_1 \\ e_2 \end{bmatrix} + \frac{1}{2} \begin{bmatrix} e_1^T, & e_2^T \end{bmatrix} \begin{bmatrix} -k_1 e_1 \\ -k_2 e_2 \end{bmatrix}$$

$$= -[k_1 e_1^T e_1 + k_2 e_2^T e_2]$$

$$= -[k_1 (e_{11}^2 + e_{12}^2 + \cdots + e_{1n}^2) + k_2 (e_{21}^2 + e_{22}^2 + \cdots + e_{2m}^2)] < 0 \ .$$

Therefore, according to Lyapunov stability theory, the error system (6.12) is asymptotically stable i.e., $\lim_{t\to\infty}\|e(t)\| = 0$. Hence, the dual combination synchronization of six complex chaotic systems is achieved by choosing appropriate controller function using nonlinear control method.

6.4 Systems' descriptions

6.4.1 Complex Lorenz system

E. N. Lorenz proposed the chaotic system in 1963, which was first of its kind. Then Flower et al. (1982) introduced the complex Lorenz system, and its dynamical property was studied by Mahmoud et al. (2007a). This system is useful to describe and simulate the physics of liquid flows. The complex Lorenz system is expressed as

$$\dot{x}'_{11} = a_1(x'_{12} - x'_{11}) \ ,$$

$$\dot{x}'_{12} = a_2\, x'_{11} - x'_{12} - x'_{11}\, x'_{13} \ ,$$

$$\dot{x}'_{13} = \frac{1}{2}(\bar{x}'_{11}\, x'_{12} + x'_{11}\, \bar{x}'_{12}) - a_{13}\, x'_{13} \ , \tag{6.14}$$

where $x'_1 = [x'_{11},\ x'_{12},\ x'_{13}]^T$ is the state vector, $x'_{11} = x_{11} + i\, x_{12}$ and $x'_{12} = x_{13} + i\, x_{14}$ are complex vectors, and $x'_{13} = x_{15}$ is real variable. The system (6.14) can be written as

$$\dot{x}_{11} = a_1(x_{13} - x_{11}) \ ,$$

$$\dot{x}_{12} = a_1(x_{14} - x_{12}) \ ,$$

$$\dot{x}_{13} = a_2\, x_{11} - x_{13} - x_{11}\, x_{15} \ ,$$

$$\dot{x}_{14} = a_2\, x_{12} - x_{14} - x_{12}\, x_{15} \ ,$$

$$\dot{x}_{15} = x_{11}\, x_{13} + x_{12}\, x_{14} - a_3\, x_{15} \ . \tag{6.15}$$

For the parameters $a_1 = 10,\ a_2 = 180,\ a_3 = 1$ and initial condition $x_1(0) = [2+3i,\ 5+6i,\ 9]^T$, the system (6.15) possesses the chaotic attractor which is described through Figure 6.1.

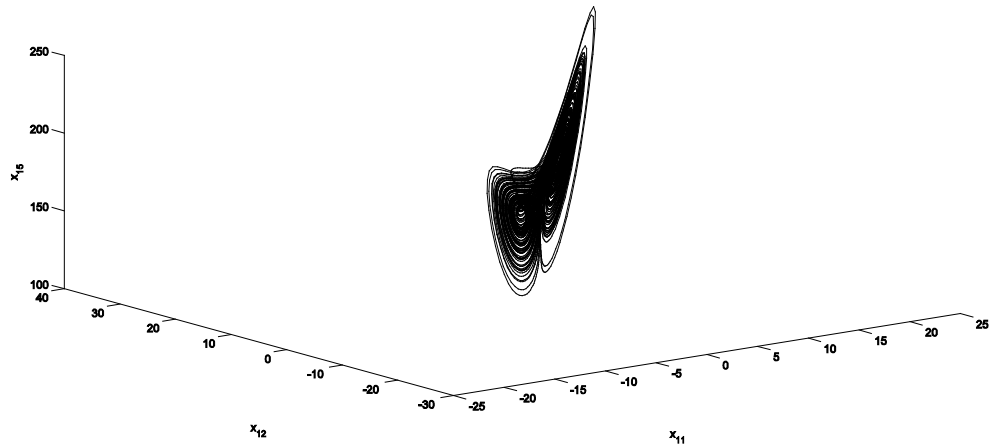

Figure 6.1 (a)

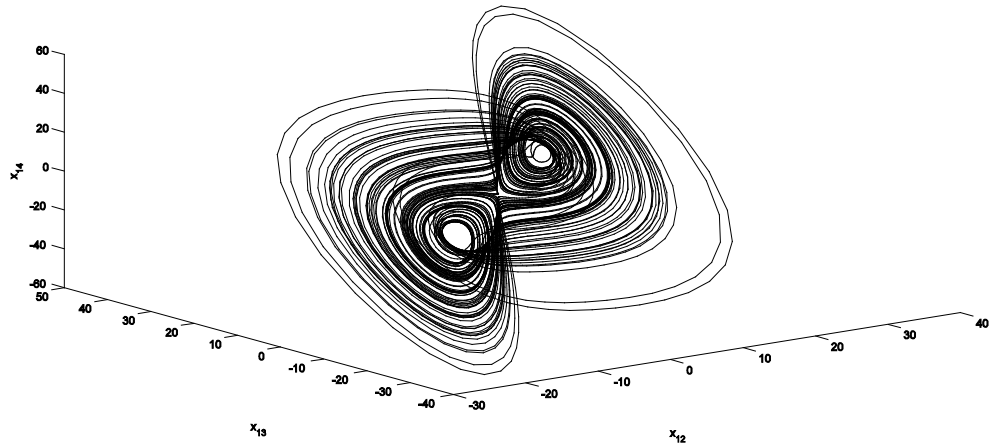

Figure 6.1 (b)

Figure 6.1: Phase portraits of the complex Lorenz system in **(a)** $x_{11} - x_{12} - x_{15}$ space, and **(b)** $x_{12} - x_{13} - x_{14}$ space.

6.4.2 Complex Lu systems

Lu and Chen introduced a chaotic system in 2002, which is known as Lu system. Mahmoud et al. (2007c) studied synchronization between complex Chen system and complex Lu system. The complex Lu system is given by

$$\dot{x}'_{21} = b_1(x'_{22} - x'_{21}) ,$$

$$\dot{x}'_{22} = b_2\, x'_{22} - x'_{21}\, x'_{23} ,$$

$$\dot{x}'_{23} = \frac{1}{2}(\bar{x}'_{21}\, x'_{22} + x'_{21}\, \bar{x}'_{22}) - b_3\, x'_{23} , \tag{6.16}$$

where $x'_2 = [x'_{21},\, x'_{22},\, x'_{23}]^T$ is the state vector variable, $x'_{21} = x_{21} + i\, x_{22}$ and $x'_{22} = x_{23} + i\, x_{24}$ are complex variables while $x'_{23} = x_{25}$ is real variable. Separating into real and imaginary parts of system (6.16), it is obtained as

$$\dot{x}_{21} = b_1(x_{23} - x_{21}) ,$$

$$\dot{x}_{22} = b_1(x_{24} - x_{22}) ,$$

$$\dot{x}_{23} = b_2\, x_{23} - x_{21}\, x_{25} ,$$

$$\dot{x}_{24} = b_2\, x_{24} - x_{22}\, x_{25} ,$$

$$\dot{x}_{25} = x_{21}\, x_{23} + x_{22}\, x_{24} - b_3\, x_{25} . \tag{6.17}$$

Figure 6.2 shows the chaotic attractors of the system for the values of parameters $b_1 = 29,\ b_2 = 21,\ b_3 = 2$ and initial condition $x_2(0) = [4 + 19i,\ 9 + 30i,\ 36]^T$.

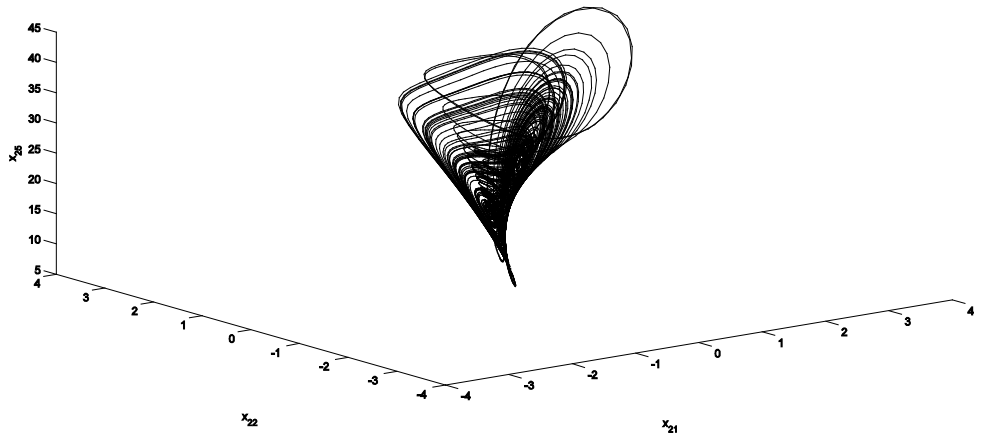

Figure 6.2 (a)

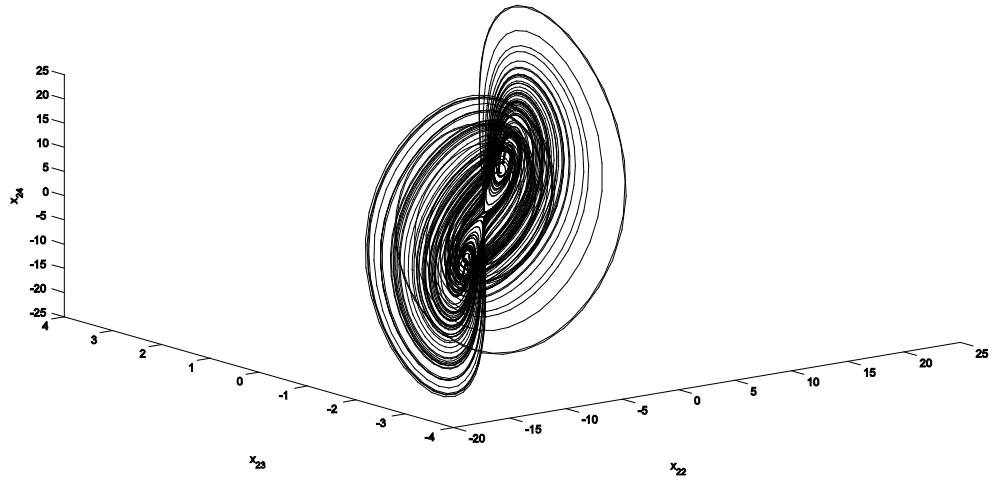

Figure 6.2 (b)

Figure 6.2: Phase portraits of the complex Lu system in **(a)** $x_{21} - x_{22} - x_{25}$ space, and **(b)** $x_{22} - x_{23} - x_{24}$ space.

6.4.3 Complex T system

Tigan and Opris (2008) proposed a 3D chaotic system, which is called T system. Later, its dynamical behaviour was studied in details by Liu et al. (2014). The complex T system is given by

$$\dot{y}_1' = c_1(y_{12}' - y_{11}') ,$$

$$\dot{y}_{12}' = (c_2 - c_1)\, y_{11}' - c_1\, y_{11}'\, y_{13}' ,$$

$$\dot{y}_{13}' = \frac{1}{2}(\bar{y}_{11}'\, y_{12}' + y_{11}'\, \bar{y}_{12}') - c_3\, y_{13}' , \tag{6.18}$$

where $y_1' = [y_{11}', y_{12}', y_{13}']^T$ is the state variable vector of the system, $y_{11}' = y_{11} + i\, y_{12}$ and $y_{12}' = y_{13} + i\, y_{14}$ are complex variables, $y_{13}' = y_{15}$ is real variable and c_1, c_2, c_3 are parameters. System (6.18) can be re-written in the following form

$$\dot{y}_1 = c_1(y_{13} - y_{11}) ,$$

$$\dot{y}_{12} = c_1(y_{14} - y_{12}) ,$$

$$\dot{y}_{13} = (c_2 - c_1)y_{11} - c_1\, y_{11}\, y_{15} ,$$

$$\dot{y}_{14} = (c_2 - c_1)y_{12} - c_1\, y_{12}\, y_{15} ,$$

$$\dot{y}_{15} = y_{11}\, y_{13} + y_{12}\, y_{14} - c_3\, y_{15} . \tag{6.19}$$

This system possesses a chaotic attractor as shown in Figure 6.3, when the parameters are taken as $c_1 = 2.1,\ c_2 = 30,\ c_3 = 0.6$ and initial condition $y_1(0) = [8 + 7i,\ 5 + 6i,\ 10]^T$.

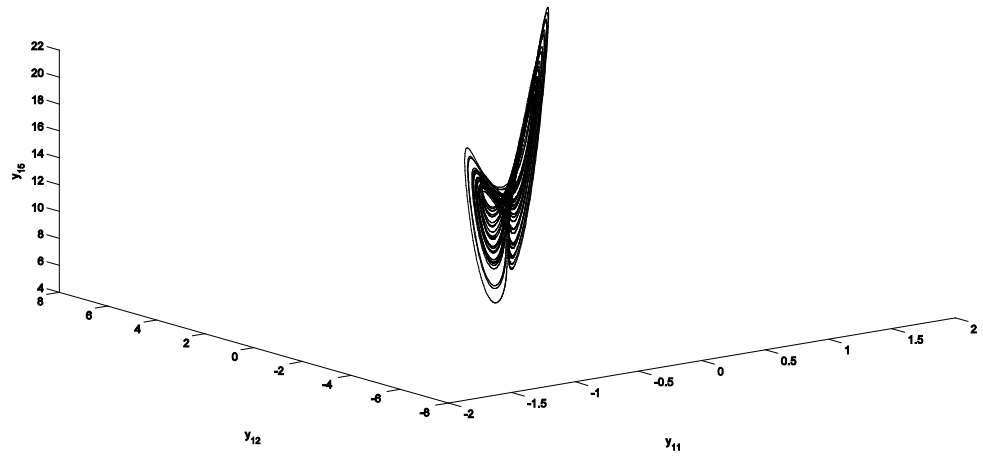

Figure 6.3 (a)

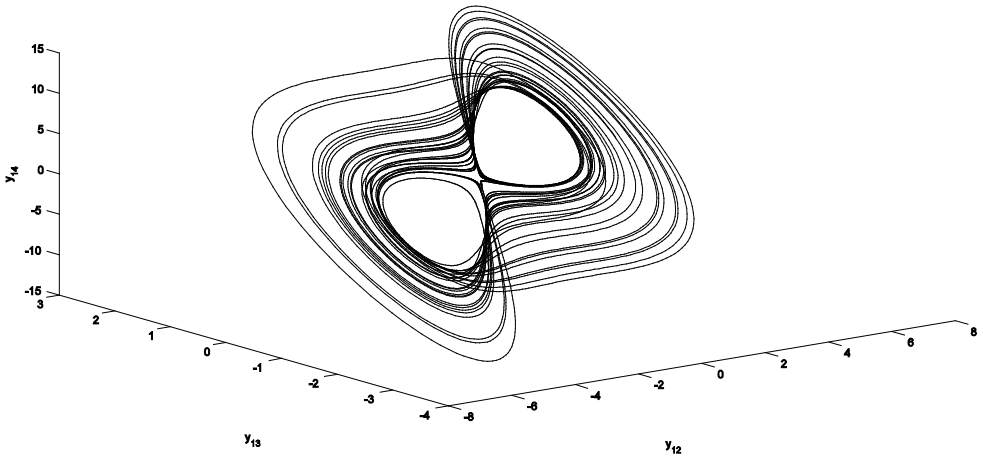

Figure 6.3 (b)

Figure 6.3: Phase portraits of the complex T system in **(a)** $y_{11} - y_{12} - y_{15}$ space, and **(b)** $y_{12} - y_{13} - y_{14}$ spaces.

6.4.4 Complex Chen system

Chen and Ueta (1999) introduced a new chaotic system, which is called Chen system. Mahmoud et al. (2009) studied synchronization between complex Chen system and complex Lu system. The complex Chen system is written as follows

$$\dot{y}'_{21} = d_1(y'_{22} - y'_{21}) ,$$

$$\dot{y}'_{22} = (d_3 - d_1)y'_{21} - y'_{21}\, y'_{23} + d_3\, y'_{22} ,$$

$$\dot{y}'_{23} = \frac{1}{2}(\bar{y}'_{21}\, y'_{22} + y'_{21}\, \bar{y}'_{22}) - d_2\, y'_{23} , \tag{6.20}$$

where $y'_2 = [y'_{21}, y'_{22}, y'_{23}]^T$ is the state variable vector of the system, $y'_{21} = y_{21} + i\, y_{22}$ and $y'_{22} = y_{23} + i\, y_{24}$ are complex variables, $y'_{23} = y_{25}$ is real variable and d_1, d_2, d_3 are parameters. From system (6.20), one can easily find the following system

$$\dot{y}_{21} = d_1(y_{23} - y_{21}) ,$$

$$\dot{y}_{22} = d_1(y_{24} - y_{22}) ,$$

$$\dot{y}_{23} = (d_3 - d_1)y_{21} - y_{21}\, y_{25} + d_3\, y_{23} ,$$

$$\dot{y}_{24} = (d_3 - d_1)y_{22} - y_{22}\, y_{25} + d_3\, y_{24} ,$$

$$\dot{y}_{25} = y_{21}\, y_{23} + y_{22}\, y_{24} - d_2\, y_{25} . \tag{6.21}$$

The chaotic behaviour of system (6.21) can be realised through Figure 6.4 when the parametric values are $d_1 = 27$, $d_2 = 1$, $d_3 = 23$, and initial condition is $y_2(0) = [-3 - 2i, -1 - 5i, -4]^T$.

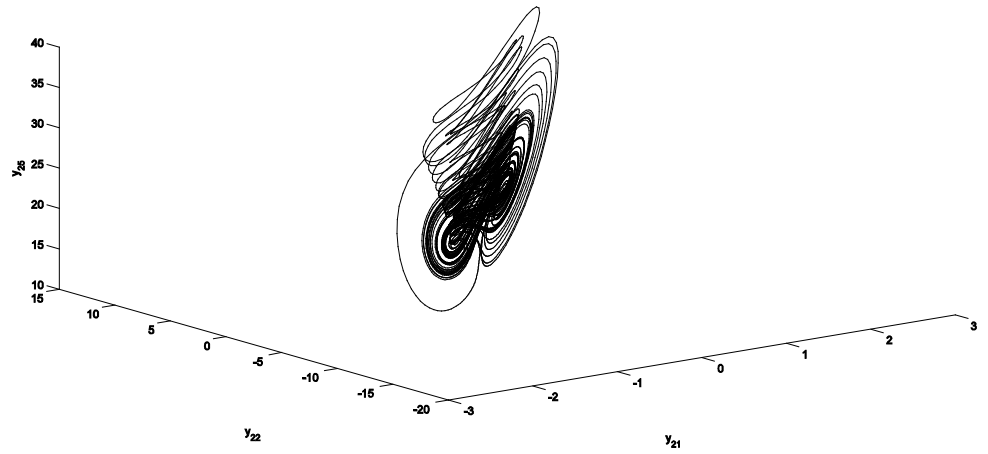

Figure 6.4 (a)

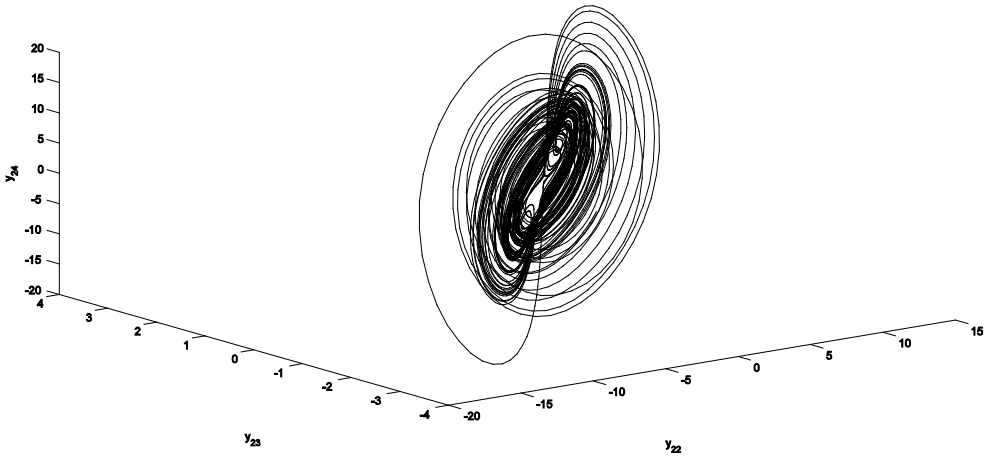

Figure 6.4 (b)

Figure 6.4: Phase portraits of the complex Chen system in **(a)** $y_{21} - y_{22} - y_{25}$ space, and **(b)** $y_{22} - y_{23} - y_{24}$ space.

6.4.5 Complex two coupled dynamos system

The real two coupled dynamos system was studied by Agiza (2002). Mahmoud et al. (2007b) studied the chaotic behaviour and chaos synchronization of a complex two coupled dynamos system which is described as

$$\dot{z}'_{11} = -l_1\, z'_{11} + z'_{12}(z'_{13} + l_2)\ ,$$

$$\dot{z}'_{12} = -l_1\, z'_{12} + z'_{11}(z'_{13} - l_2)\ ,$$

$$\dot{z}'_{13} = 1 - \frac{1}{2}(\bar{z}'_{11}\, z'_{12} + z'_{11}\, \bar{z}'_{12})\ , \tag{6.22}$$

where $z'_1 = [z'_{11}\,,\ z'_{12}\,,\ z'_{13}]^T$ is the vector of state variables, $z'_{11} = z_{11} + i\, z_{12}$ and $z'_{12} = z_{13} + i\, z_{14}$ are complex variables, and $z'_{13} = z_{15}$ is real variable. Splitting system (6.22) into real and imaginary parts, it is obtained as

$$\dot{z}_{11} = -l_1\, z_{11} + l_2\, z_{13} + z_{13}\, z_{15}\ ,$$

$$\dot{z}_{12} = -l_1\, z_{12} + l_2\, z_{14} + z_{14}\, z_{15}\ ,$$

$$\dot{z}_{13} = -l_2\, z_{11} - l_1\, z_{13} + z_{11}\, z_{15}\ ,$$

$$\dot{z}_{14} = -l_2\, z_{12} - l_1\, z_{14} + z_{12}\, z_{15}\ ,$$

$$\dot{z}_{15} = 1 - z_{11}\, z_{13} - z_{12}\, z_{14}\ . \tag{6.23}$$

Figure 6.5 shows the chaotic attractors of system (6.23) if parameters are taken as $l_1 = 0.8,\ l_2 = 1.8$, and initial condition $z_1 = [-3 + 2i\,,\ -1 + 2i\,,\ -1]^T$.

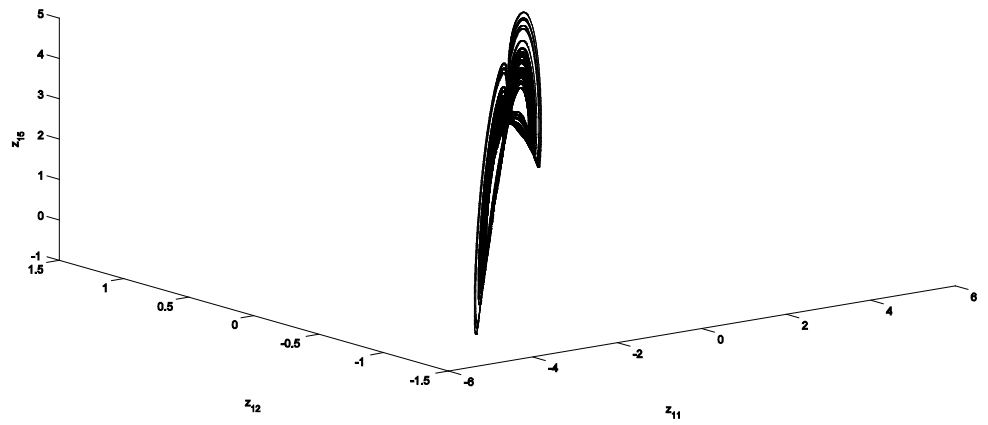

Figure 6.5 (a)

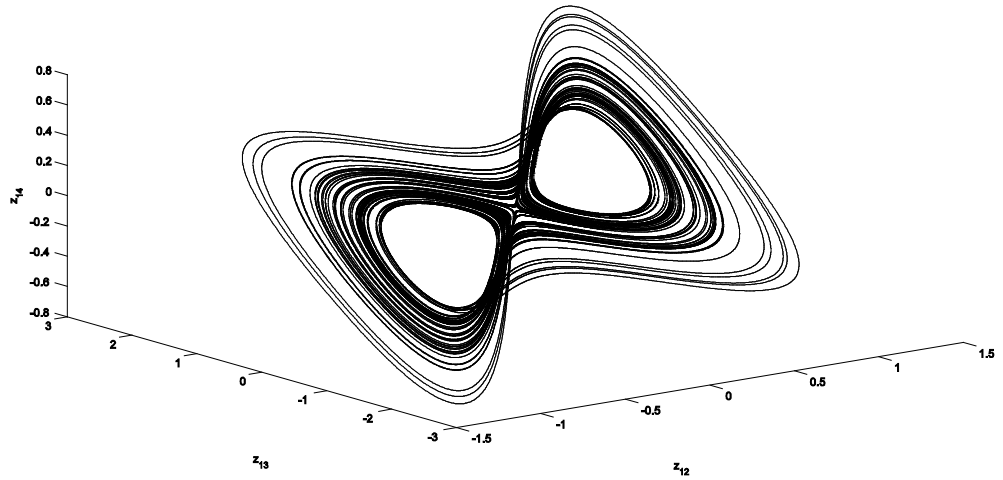

Figure 6.5 (b)

Figure 6.5: Phase portraits of the complex two coupled system in **(a)** $z_{11} - z_{12} - z_{15}$ space, and **(b)** $z_{12} - z_{13} - z_{14}$ space.

6.4.6 Nonlinear complex chaotic system

Recently, Sun et al. (2016b) designed a novel nonlinear complex chaotic system, whose real counterpart was studied by Muthuswamy and Chua (2010). This complex chaotic system is written as follows

$$\begin{aligned}
\dot{z}'_{21} &= m_1 z'_{22} z'_{23} , \\
\dot{z}'_{22} &= m_2 (z'_{21} - z'_{22}) , \\
\dot{z}'_{23} &= 1 - z'_{21} \bar{z}'_{21} ,
\end{aligned} \tag{6.24}$$

where $z'_2 = [z'_{21}, z'_{22}, z'_{23}]^T$ is the vector of state variables, $z'_{21} = z_{21} + i z_{22}$ and $z'_{22} = z_{23} + i z_{24}$ are complex variables while $z'_{23} = z_{25}$ is real variable. System (6.24) can written as

$$\begin{aligned}
\dot{z}_{21} &= m_1 z_{23} z_{25} , \\
\dot{z}_{22} &= m_1 z_{24} z_{25} , \\
\dot{z}_{23} &= m_2 (z_{21} - z_{23}) , \\
\dot{z}_{24} &= m_2 (z_{22} - z_{24}) , \\
\dot{z}_{25} &= 1 - z_{21}^2 + z_{22}^2 .
\end{aligned} \tag{6.25}$$

For parameters $m_1 = 1$, $m_2 = 1$ and initial conditions $z_2(0) = [0.1 + 0.1i, -0.3 - 0.4i, 0.5]^T$, the system (6.25) possesses the chaotic attractor shown through Figure 6.6.

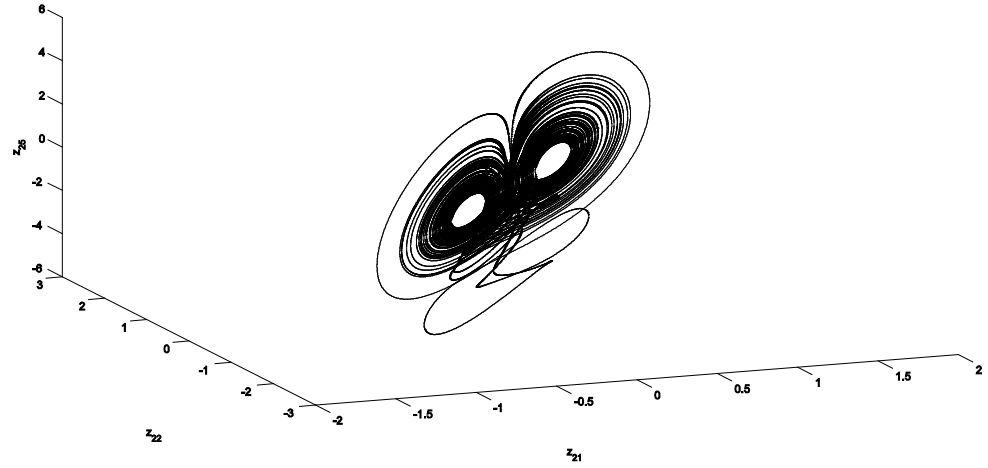

Figure 6.6 (a)

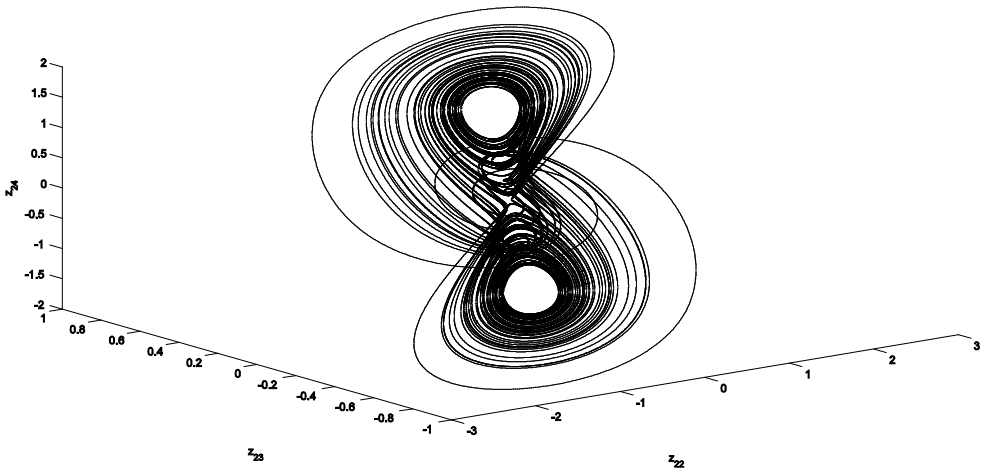

Figure 6.6 (b)

Figure 6.6: Phase portraits of the nonlinear complex chaotic system in **(a)** $z_{21} - z_{22} - z_{25}$, and **(b)** $z_{22} - z_{23} - z_{24}$ spaces.

6.5 Illustration of the scheme

An illustration of the scheme for dual combination synchronization is presented in this section, so that one can realised the effectiveness of the proposed scheme. To achieve our aim, the four realise systems described in (6.14), (6.17), (6.19) and (6.21) are considered as drive systems. Systems (6.23) and (6.25) are taken as two response systems. Therefore, response systems are obtained as

$$\dot{z}_{11} = -l_1\, z_{11} + l_2\, z_{13} + z_{13}\, z_{15} + u_{11}\ ,$$

$$\dot{z}_{12} = -l_1\, z_{12} + l_2\, z_{14} + z_{14}\, z_{15} + u_{12}\ ,$$

$$\dot{z}_{13} = -l_2\, z_{11} - l_1\, z_{13} + z_{11}\, z_{15} + u_{13}\ ,$$

$$\dot{z}_{14} = -l_2\, z_{12} - l_1\, z_{14} + z_{12}\, z_{15} + u_{14}\ ,$$

$$\dot{z}_{15} = 1 - z_{11}\, z_{13} - z_{12}\, z_{14} + u_{15}\ , \tag{6.26}$$

and

$$\dot{z}_{21} = m_1\, z_{21}\, z_{25} + u_{21}\ ,$$

$$\dot{z}_{22} = m_1\, z_{22}\, z_{25} + u_{22}\ ,$$

$$\dot{z}_{23} = m_2 (z_{21} - z_{23}) + u_{23}\ ,$$

$$\dot{z}_{24} = m_2 (z_{22} - z_{24}) + u_{24}\ ,$$

$$\dot{z}_{25} = 1 - z_{21}^2 + z_{22}^2 + u_{25}\ . \tag{6.27}$$

For the convenience of the ensuing discussion, let us take $A = B = C = P = Q = R = I$ and $k_1 = k_2 = 1$. Control functions are obtained based on the system (6.11), in the following form

$$u_{11} = l_1 z_{11} - l_2 z_{13} - z_{13} z_{15} + a_1(x_{13} - x_{11}) + c_1(y_{13} - y_{11}) + e_{11} ,$$

$$u_{12} = l_1 z_{12} - l_2 z_{14} - z_{14} z_{15} + a_1(x_{14} - x_{12}) + c_1(y_{14} - y_{12}) + e_{12} ,$$

$$u_{13} = l_2 z_{11} + l_1 z_{13} - z_{11} z_{15} + a_2 x_{11} - x_{13} - x_{11} x_{15} + (c_2 - c_1) y_{11} - c_1 y_{11} y_{15} + e_{13} ,$$

$$u_{14} = l_2 z_{12} + l_1 z_{14} - z_{12} z_{15} + a_2 x_{12} - x_{14} - x_{12} x_{15} + (c_2 - c_1) y_{12} - c_1 y_{12} y_{15} + e_{14} ,$$

$$u_{15} = -1 + z_{11} z_{13} + z_{12} z_{14} + x_{11} x_{13} + x_{12} x_{14} - a_3 x_{15} + y_{11} y_{13} + y_{12} y_{14} - c_3 y_{15} + e_{15} , \quad (6.28)$$

and

$$u_{21} = -m_1 z_{23} z_{25} + b_1(x_{23} - x_{21}) + d_1(y_{23} - y_{21}) + e_{21} ,$$

$$u_{22} = -m_1 z_{24} z_{25} + b_1(x_{24} - x_{22}) + d_1(y_{24} - y_{22}) + e_{22} ,$$

$$u_{23} = -m_2(z_{21} - z_{23}) + b_2 x_{23} - x_{21} x_{25} + (d_3 - d_1) y_{21} - y_{21} y_{25} + d_3 y_{23} + e_{23} ,$$

$$u_{24} = -m_2(z_{22} - z_{24}) + b_2 x_{24} - x_{22} x_{25} + (d_3 - d_1) y_{22} - y_{22} y_{25} + d_3 y_{24} + e_{24} ,$$

$$u_{25} = -1 + z_{21}^2 - z_{22}^2 + x_{21} x_{23} + x_{22} x_{24} - b_3 x_{25} + y_{21} y_{23} + y_{22} y_{24} - d_2 y_{25} + e_{25} . \quad (6.29)$$

The control functions are designed according to Theorem 6.2. Therefore response systems (6.28) and (6.29) keep the same trajectories, as drive systems (6.15), (6.17), (6.19), (6.21) and as a result the dual combination synchronization amongst chaotic systems (6.15), (6.17), (6.19), (6.21), (6.28) and (6.29) are achieved.

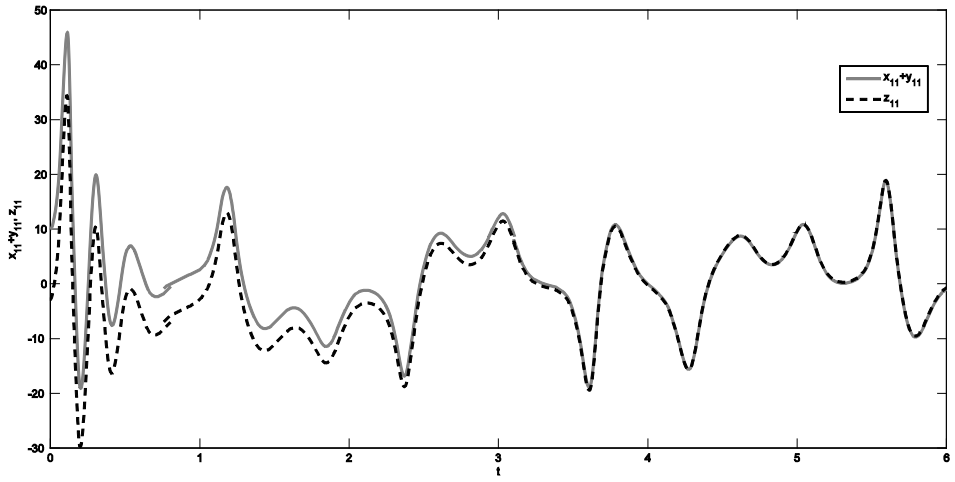

Figure 6.7 (a)

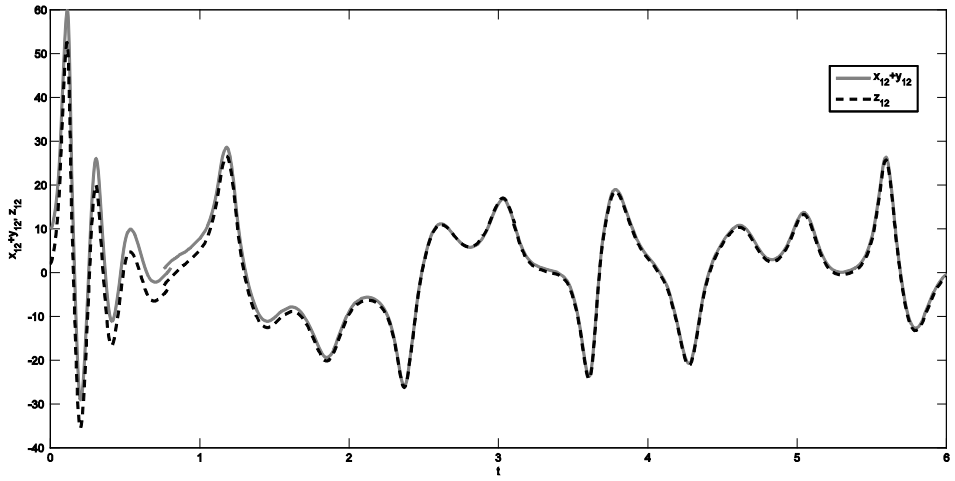

Figure 6.7 (b)

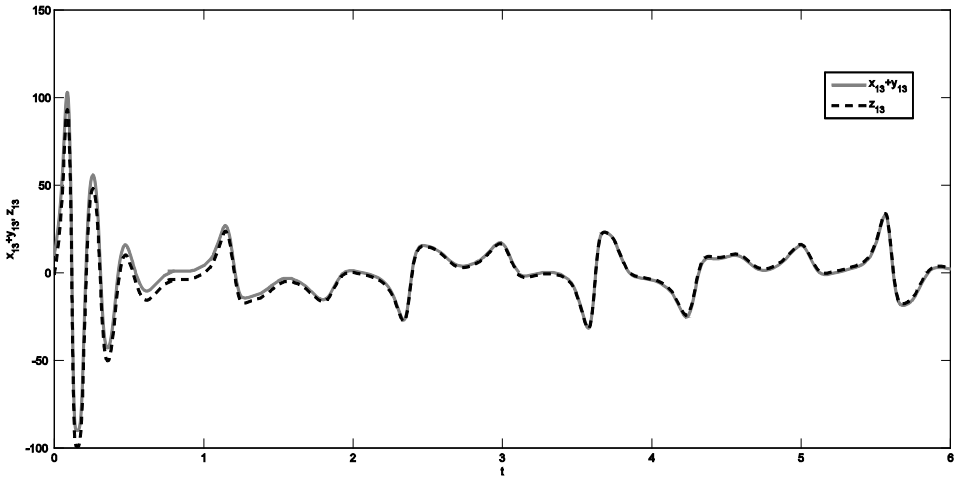

Figure 6.7 (c)

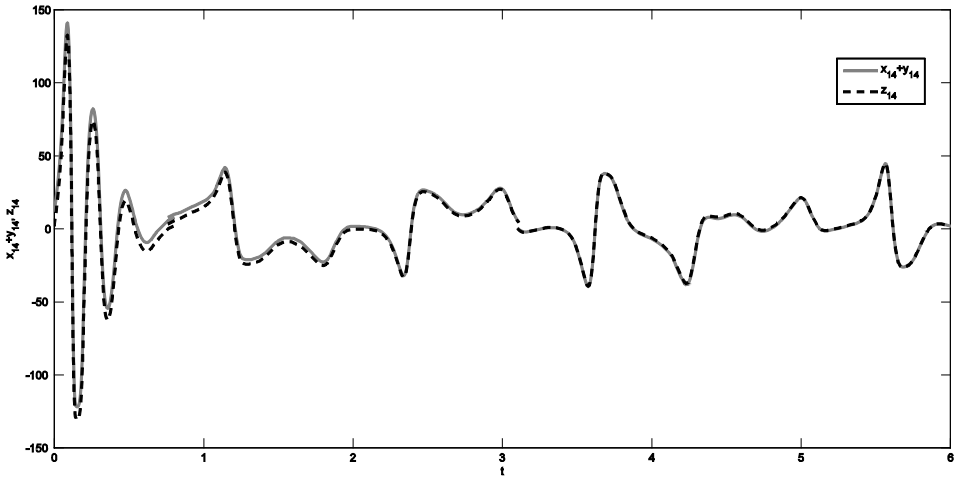

Figure 6.7 (d)

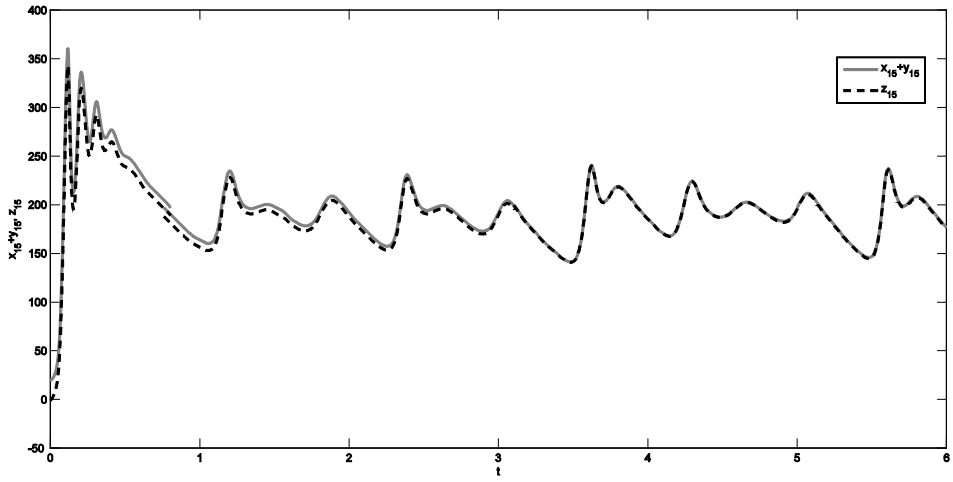

Figure 6.7 (e)

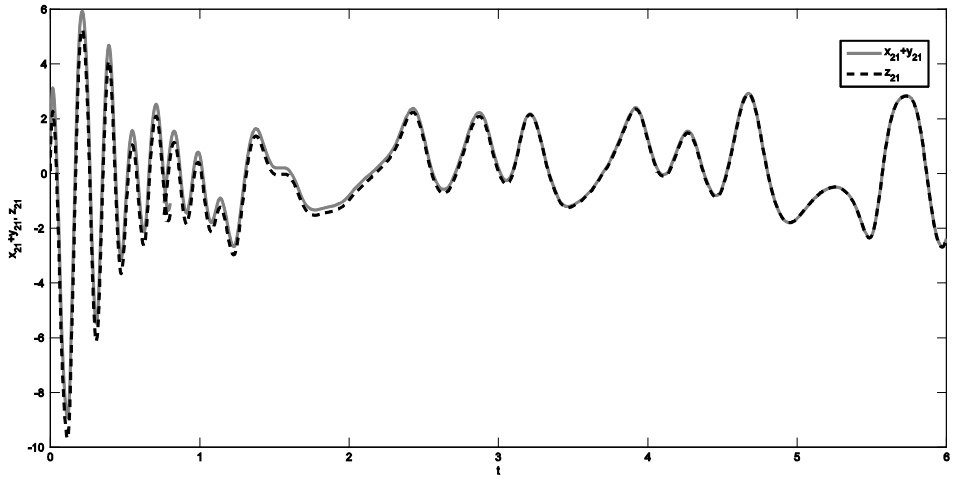

Figure 6.7 (f)

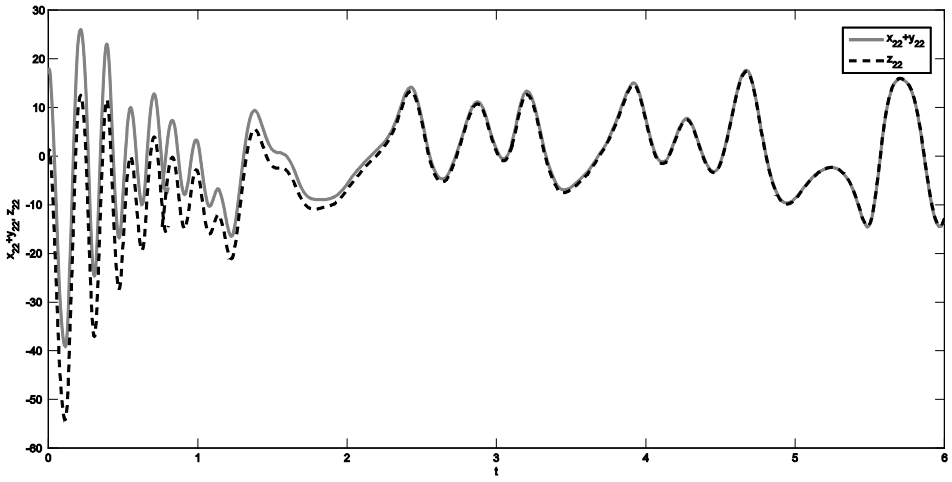

Figure 6.7 (g)

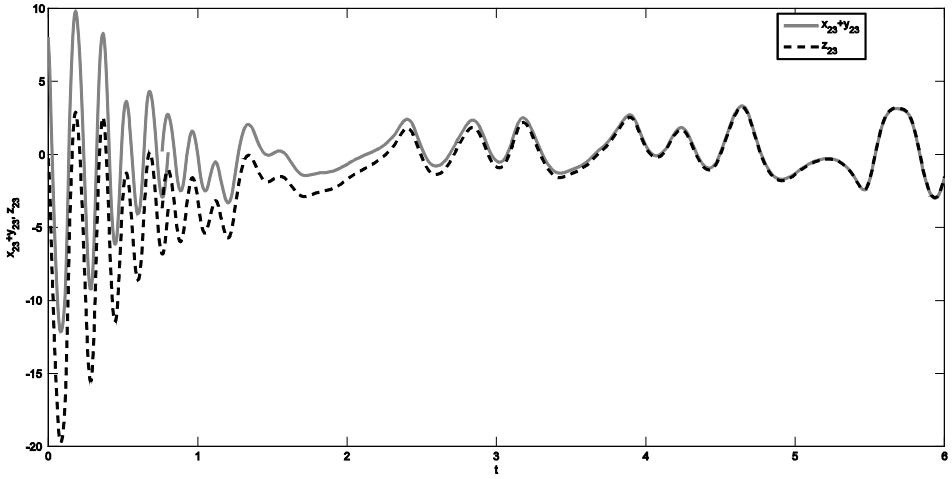

Figure 6.7 (h)

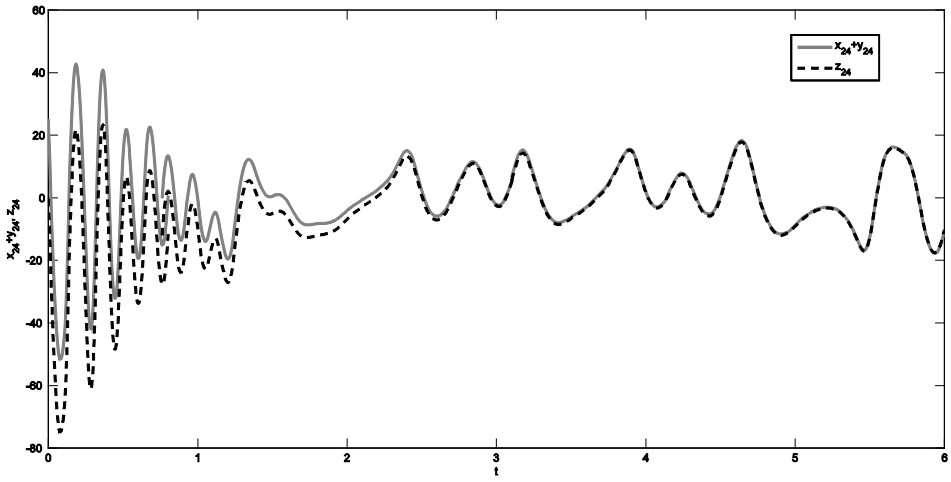

Figure 6.7 (i)

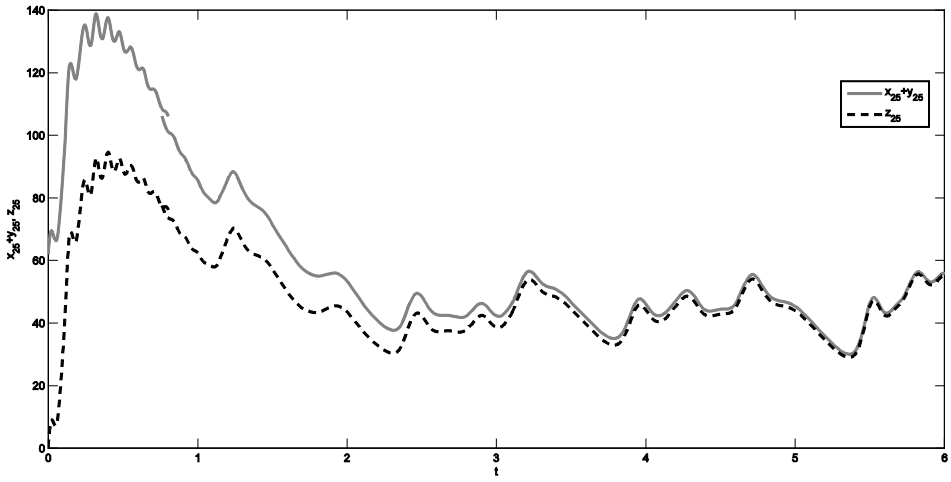

Figure 6.7 (j)

Figure 6.7: State trajectories of the complex chaotic systems (6.15), (6.17), (6.19), (6.21), (6.26) and (6.27) between : **(a)** $x_{11}(t)+y_{11}(t)$ and $z_{11}(t)$; **(b)** $x_{12}(t)+y_{12}(t)$ and $z_{12}(t)$; **(c)** $x_{13}(t)+y_{13}(t)$ and $z_{13}(t)$; **(d)** $x_{14}(t)+y_{14}(t)$ and $z_{14}(t)$; **(e)** $x_{15}(t)+y_{15}(t)$ and $z_{15}(t)$; **(f)** $x_{21}(t)+y_{21}(t)$ and $z_{21}(t)$; **(g)** $x_{22}(t)+y_{22}(t)$ and $z_{22}(t)$; **(h)** $x_{23}(t)+y_{23}(t)$ and $z_{23}(t)$; **(i)** $x_{24}(t)+y_{24}(t)$ and $z_{24}(t)$; **(j)** $x_{25}(t)+y_{25}(t)$ and $z_{25}(t)$.

6.6 Simulation results and discussion

In this section, the feasibility of the proposed scheme have been demonstrated. The fourth-order Runge–Kutta algorithm is used with time step size 0.001. During simulation, the values of all the parameters remain unchanged and the initial conditions are also taken as before. Hence, the initial error is $[e_{11}+ie_{12}, e_{13}+ie_{14}, e_{15}, e_{21}+ie_{22}, e_{23}(t)+ie_{24}(t), e_{25}]^T = [13+8i,\ 11+10i,\ 20,\ 0.9+16.9i,\ 8.3+25.4i,\ 31.5]^T$. Figures 6.7 (a)–(e) display the time responses of the states $x_{1j}(t)+y_{1j}(t)$ and $z_{1j}(t)$ of the drive systems (6.15), (6.17), (6.19), (6.21) and the response systems (6.26), (6.27) for $j=1(1)5$. The similar things between the states $x_{2j}(t)+y_{2j}(t)$ and $z_{2j}(t)$ of drive systems and response systems are depicted through Figures 6.7(f)–(j) for $j=1(i)5$. Figure 6.8 shows that the error vectors asymptotically converge to zero as time becomes large which implies that dual combination synchronizations amongst the considered chaotic systems are achieved.

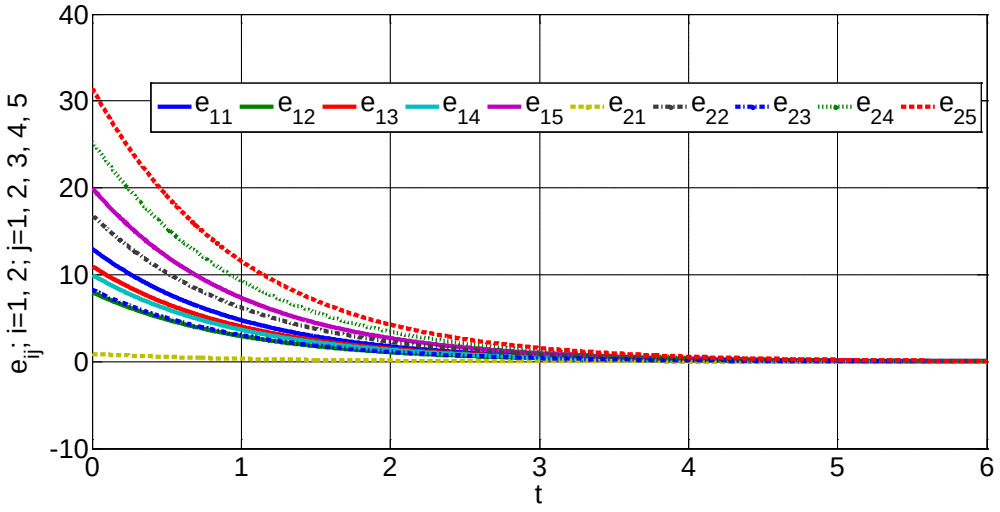

Figure 6.8: The plot for the evaluation of error functions $e_{ij}(t)$, $i=1,2$; $j=1,2,\cdots,5$.

6.7 Conclusion

In this chapter, a novel scheme of dual combination synchronization of six distinct complex chaotic systems in which four drive and two response systems, is proposed based on Lyapunov stability theory. A validation of the generalization of the proposed scheme over the other useful synchronization schemes is an important achievement of the present scientific contribution.

*****